Short review of dental microstructure and dental microwear in xenarthran teeth

Daniela C. Kalthoff

Introduction

Dentin is one of three tooth tissues occurring in mammals, the other two being the hypermineralized tooth enamel and tooth cementum. In respect to volume, dentin usually makes up the largest part of the tooth. Interestingly, a number of mammal taxa have reduced the resistant layer of tooth enamel during their evolutionary history, thus focusing on dentin as the main tooth building tissue. Enamelless teeth can be found in various extant and extinct taxa of odontocete whales (Odontoceti), aardvarks (Tubulidentata), armadillos, glyptodonts and pampatheres (Cingulata), sloths (Folivora), walruses (Odobenidae), sea cows (Dugongidae), and elephants (Proboscidea).

This review will give an overview of recent results on histology as well as dietary adaptations using the distinctly built dentin teeth in armadillos and sloths and their fossil relatives (in the following referred to with the informal term "xenarthran(s)"). Toothed xenarthrans show an astonishing diversity regarding tooth shapes (e.g., complex to simplified; Fig. 12.1) and number of teeth (severely reduced to abundant supernumerary teeth).

Afrotheria, Laurasiatheria, Euarchontoglires, and Xenarthra are the four major clades within placental mammals (Murphy et al. 2001, O'Leary et al. 2013). Showing unique characters in e.g., skeletal morphology and life history traits, both extinct and extant xenarthrans are well investigated and even have experienced increased scientific attention in the last two decades (e.g., Fariña et al. 2003, 2013, Vizcaíno & Loughry 2008, Bargo & Nyakatura 2018). On the other hand, research on dental histology in this group is rather meagre. Historically, studies on xenarthran dentin date back to the first half of the 19th century (Retzius 1837, Owen 1840–1845, Owen 1842). Only 80 years later, some more papers were published (Schmidt 1924, Arsuffi 1938, Schmidt & Keil 1958, Keil & Venema 1963), all focusing on one or few taxa and not revealing dentin microstructure in necessary detail, mainly because all these studies relied on light microscopy. Ferigolo (1985) was the first investigating a larger number of both fossil and extant species and also the first one applying scanning electron microscopy (SEM).

Also using SEM technique, the most comprehensive and detailed histological study to date is from Kalthoff (2011), comprising teeth from about 50 xenarthran taxa dating from late Eocene to Holocene.

Dental microwear analysis is the study of microscopic scars on the chewing surface of cheek teeth. Last consumed food items (and potentially also exogenous grit; Hoffman et al. 2015) leave these scars, mainly different kinds of pits and scratches, during mastication and different food categories (leaves, grass, seeds, fruits, meat, insects, etc.) produce different kinds of scars. Extant species with known diets are used to calibrate microwear scars. From the beginning of dental microwear analysis, the highly mineralized enamel had been the target tissue, and this technique has been employed to various mammal clades (e.g., Walker 1976, Walker et al. 1978, Rensberger 1978, Teaford 1991, Semprebon et al. 2004), but has also been used to recognize dietary adaptations in other vertebrates such as reptiles and fish (e.g., Purnell et al. 2012, Winkler et al. 2019). The much softer dentin was thought not suitable to reliably record microwear features; however, this assumption was challenged and proven incorrect. Beginning with Oliveira (2001), several studies successfully applying dental microwear on dentin have been published, leading to new and exciting insights in xenarthran paleobiology (e.g., Green 2009a, b, Green & Resar 2012, Haupt et al. 2013, Resar et al. 2013, Green & Kalthoff 2015, Kalthoff & Green 2018). Thus, the analysis of dentin has been proven feasible and very interesting as independent proxy for feeding ecology in taxa with enamelless teeth.

In the following, established knowledge and recent results on dentin microstructure analysis as well as dentin microwear analysis will be reviewed. If not mentioned differently, they are based on Kalthoff (2011), Green & Kalthoff (2015), and Kalthoff & Green (2018). Appendices 1 and 2 provide an overview about specimen details and their most conspicuous characters in respect to dentin microstructure and/or dental microwear.

Preparation techniques

In the fossil record, dentin microstructures – similar as those of enamel – are usually preserved without alterations. As a general phenomenon of taphonomic processes, a tooth can be impregnated with different minerals (e.g., Mn, Fe) and thus change color, but the internal structures usually are not affected. This means that dentin of extinct and extant taxa can be analyzed with the same techniques. However, if alterations occur, they are obvious and easy to recognize, regardless whether they occurred at an early (Kalthoff et al. 2011) or later post-mortem stage.
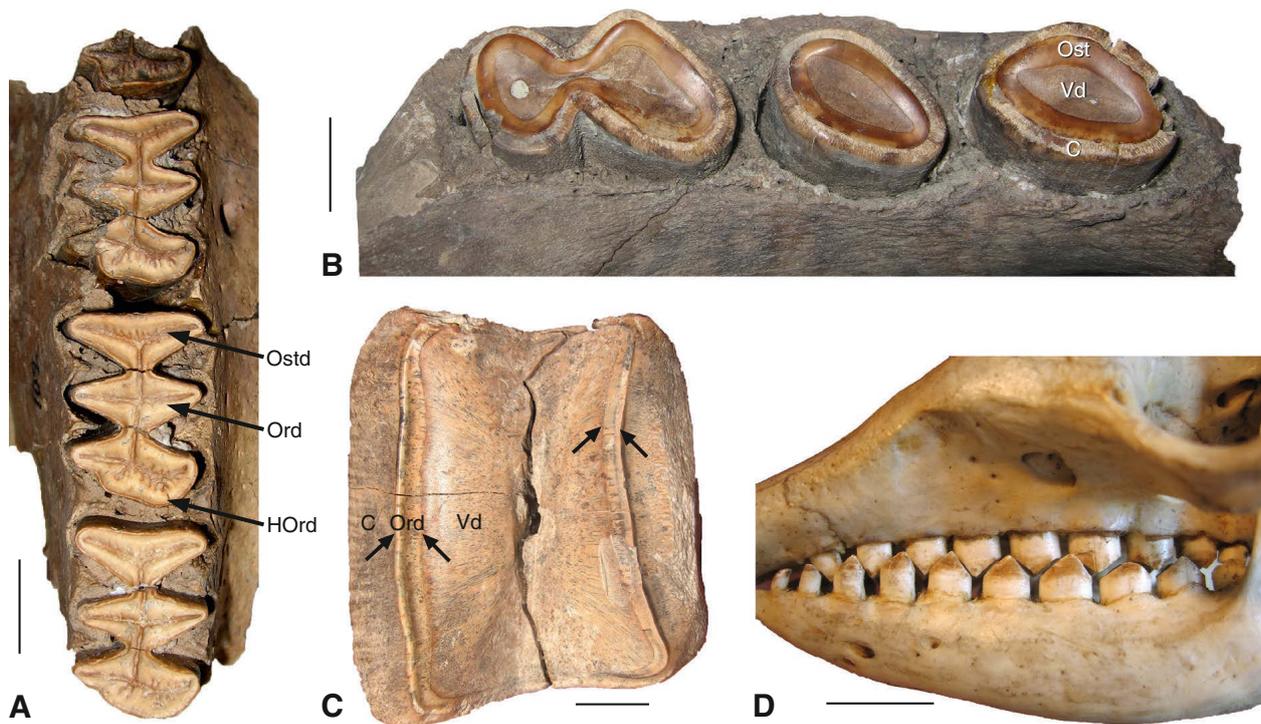
Fig. 12.1. Tooth morphology in extant and extinct xenarthrans. **A,** Left maxilla fragment of *Glyptodon clavipes* (Glyptodontidae) in occlusal view with three complete, "Christmas tree-shaped" cheek teeth (NHMD-ZMK 70/1885). The slightly darker, ramifying, and elevated material in the tooth center is osteodentin (Ostd), outward follows orthodentin (Ord), then a thin, slightly darker and elevated layer of hard orthodentin (HOrd). Rostral is up. **B,** Fragment of right mandible of *Lestodon armatus* (Mylodontidae) in oblique view from lateral with three complete molariform teeth (NHMD-ZMK 52/1888). The center layer is vasodentin (Vd), the hazelnut-brown layer orthodentin (Ord), the outer, gray-brown later is tooth cementum (C). Rostral is to the right. **C,** *Megatherium americanum* (Megatheriidae), undetermined cheek tooth (NHMD-ZMK 56/1885) in occlusal view. The thin layer between the arrows is orthodentin (Ord), forming sharp cutting edges. Outward is a thick layer of softer tooth cementum (C), the inner part is made of softer vasodentin (Vd). **D,** Left lateral view of dentition of the living six-banded armadillo *Euphractus sexcinctus* (NHMD L62). The peg-like teeth show anterior- and posterior-facing facets and interlocking of maxillary and mandibular teeth. NHMD, Natural History Museum of Denmark, Copenhagen, Denmark; NHMD-ZMK, Zoologisk Museum Kvartærzoologi (Quaternary Zoology collection), Natural History Museum of Denmark, Copenhagen. Scale bars equal 1 cm.

Dentin needs "special attention" when it comes to preparation in order to expose the full set of microstructural details. Dentin microstructures can be analyzed with transmitted light microscopy using thin sections or by scanning electron microscopy (SEM) using pseudo-3D surfaces produced through etching. In contrast to enamel, dentin is a friable tissue and easily fractured under preparation stresses. Therefore, tooth samples should be completely embedded and thus stabilized in translucent epoxy resin; for thin sectioning, it is even advised to use the resin for repeated vacuum impregnation during the different preparation steps. For SEM preparation, it has proven most advantageous to etch the trimmed surfaces with Mutvei's solution (Schöne et al. 2005). Mutvei's solution comprises (1) acetic acid for gentle and slow etching, (2) glutardialdehyde as fixation agent, and (3) alcian blue for staining. A detailed description of preparation procedures can be found in Kalthoff (2011).

Different types of dentinal tissues in xenarthran cheek teeth

In mammalian teeth, dentin (Fig. 12.2) occurs in three different varieties, namely orthodentin, vasodentin, and osteodentin. Orthodentin is the most common variety (often simply referred to as "dentin") and occurs in all mammalian teeth (regardless whether enameled or enamelless), whereas vasodentin and osteodentin are restricted to xenarthrans. Compared to the almost completely mineralized tooth enamel, the moderately porous orthodentin is much softer and elastic making it an ideal counter bearing tissue in enameled teeth. Orthodentin contains about 20 % by weight of collagenous proteins (Carlson 1990) and is not vascularized. Its microstructure is characterized by sub-parallel, slightly S-curved dentinal tubules raising radially in direction of the tooth crown in a rather homogeneous dentin matrix. Each dentinal tubule accommodates a thin cytoplasmic process, the so-called odontoblastic process or Tomes' process, and dentinal fluid. From the outer wall of the odontoblastic process protrude even thinner extensions, which normally are short and occasionally bifurcate (Fig. 12.2E). The odontoblastic process and its extensions

are commonly preserved as calcified tubes (Fig. 12.2A, E).

Orthodentin can further be split into two subtypes of different biomechanical properties: firstly, the organic matter-rich intertubular dentin, and secondly, the almost inorganic peritubular dentin (Ten Cate 1998) (Fig. 12.2C, D). Intertubular dentin makes up the dentin matrix being a network of collagenous fibers with embedded mineral crystals. In contrast, peritubular dentin is a collagen-free and highly mineralized dentinal tissue (Habelitz et al. 2007), and in this respect resembles tooth enamel. However, in contrast to the dense enamel, peritubular dentin is rather porous. Peritubular dentin is located at the inner periphery of the individual tubules (Fig. 12.2C) and assumed to be precipitated during dentinogenesis (Ten Cate 1998).

Orthodentin occurs in all xenarthrans and is the hardest dental tissue in sloths (Fig. 12.2B). Xenarthran orthodentin is microstructurally different from that of other mammals. Firstly, dentinal tubules are arranged in close proximity throughout the entire tooth height, herewith differing from e.g., human teeth in which tubule density is wider at the enamel-dentin junction (Mjör & Nordahl 1996). Secondly, individual dentinal tubules are on average wider as in other mammals, measuring up to 7 μm in, e.g., the extant three-toed sloth *Bradypus*. Both SEM and synchrotron radiation X-ray tomographic microscopy results suggest that large parts of the lumen in the wider dentinal tubules are occupied by the highly mineralized peritubular dentin (Fig. 12.2D), thus suggesting that xenarthran orthodentin is biomechanically more resistant than that of other mammals. Thirdly, in xenarthran orthodentin and here especially in sloths, the small extensions protruding from the odontoblastic process are very long, regularly reaching and piercing through the tubule wall and thereby entering the neighboring tubule. In addition, extensions show frequent branching and even are connected to each other and, as a consequence, form a dense but irregular meshwork (Fig. 12.2E). In other mammals, side-extensions are either absent (e.g., diprotodont marsupials) or fewer and shorter without forming networks (many placental mammals).

The reason behind the differing orthodentin architecture in xenarthran teeth is far from being understood and needs further investigation. As mentioned above, one possible explanation lies in the improvement of the biomechanical properties of the tooth, which evolved to counterbalance the lack of a resistant enamel layer. Alternatively, the biochemical regulating transport system of the tooth is enhanced, in which peritubular dentin plays an important role (Gotliv & Veis 2007, 2008). Both explanations can be true, of course.

A conspicuous type of orthodentin exclusively occurs in extinct cingulates (Glyptodontidae, Pampatheriidae, *Proeutatus*, *Eutatus*). It is termed 'hard orthodentin' for it forms an outer rim surrounding the tooth and thus being more wear resistant than the neighbouring 'regular orthodentin' (Figs. 1A, 2F, G). Microstructurally, the 'hard orthodentin' is undistinguishable from the regular type but μCT images reveal that the 'hard orthodentin' is optically more dense, which can be translated to being higher mineralized (Fig. 12.2G). The fact that the hard orthodentin type only occurs in fossil cingulate teeth makes it difficult to reveal the reasons for its increased hardness. Analysis of mineral composition and hardness tests by indentation seem appropriate techniques to approach this question; however, taphonomic processes have to be taken into account when interpreting the results. Still, the increased hardness is very likely to be primary because the prominent outer rim is a consistent feature.

The second dentinal tissue, true osteodentin, occurs within Mammalia exclusively in extinct cingulates (Glyptodontidae, Pampatheriidae, *Proeutatus*, *Eutatus*). This dentin variety consists of densely packed primary osteons and is permeated with blood vessels and nerves, both of which are often arranged in rows. True osteodentin is always located in the center of the tooth, followed toward the outer tooth surface by orthodentin and hard orthodentin (Fig. 12.2F, G). In glyptodontids and pampatheres, the area occupied by osteodentin is elongated and shows branching toward the convexities (Fig. 12.1A). The osteodentin area always forms the highs in the tooth relief, suggesting it being hard and resistant to abrasion. The teeth of the Miocene horned armadillo *Peltephilus*, the Pliocene armadillo *Macroeuphractus*, and, unexpectedly, also the extant three-banded armadillo *Tolypeutes*, the hairy armadillo *Chaetophractus*, and the pichi *Zaedyus*, show a swelled, central cloud-shaped region encircling a tissue, harder than the surrounding orthodentin. Although being devoid of vascularization and identifiable primary osteons, the microstructural appearance reminds of osteodentin, which is why this central tissue is interpreted as 'degenerated osteodentin'.

The third dentin variety is vasodentin (Fig. 12.2B). As the term suggests, vasodentin is vascularized and shows relatively wide vascular canals (20–25 μm on average) and an overall porous appearance. Vasodentin lacks dentinal tubules and is relatively soft, compared to orthodentin and osteodentin. It occurs as central tissue in the teeth of extant and extinct sloths (Fig. 12.1B, C) and some living armadillos such as *Dasypus*. Vasodentin is absent in fossil cingulates and it has never been proven to be present in any other mammal.

The so-called "globular dentin" of the walrus *Odobenus rosmarus* (Kastelein 2009) is currently under study by the author.

Form and function of xenarthran cheek teeth

Xenarthran teeth are unusual in several aspects. Above, it has already been mentioned that they generally are devoid of enamel; despite the great systematic diversity of fossil xenarthrans, only two Eocene armadillo species show remnants of enamel (Simpson 1932; Ciancio et al. 2014), likewise do the milk teeth of the extant genus *Dasypus* (Martin 1916). The reasons for xenarthran teeth becoming enamelless are still not solved, however, the fossil record in armadillos shows that this happened synchronous with teeth becoming rootless and continuously growing. To date, no fossil sloth teeth with an outer enamel coating have been discovered.

Genetic studies suggest that reduction and loss of enamel occurred independently in cingulates and folivores (Meredith et al. 2009). This result makes sense in the light of their different strategies of dentin tissue organization: in sloths and their fossil relatives (Folivora), we see a layered composition of a central vasodentin core, which is surrounded by a thick orthodentin layer, followed by an outer collar of cementum (Figs. 1B, 2B). In this make-up, orthodentin is the most wear-resistant (= hard) layer forming the highest rims of the tooth, while vasodentin and cementum are comparably less wear-resistant (= soft). By contrast, fossil cingulates combine an inner layer of osteodentin (or 'degenerated osteodentin' in some taxa, see above), surrounded by orthodentin as middle layer and followed by an outer layer of 'hardened orthodentin' (Figs. 1A, 2F, G). In this make-up, both osteodentin types and the 'hardened orthodentin' are the most wear-resistant, rim-forming tissues (= very hard) while the regular orthodentin is comparably less wear-resistant (= less hard). Living armadillos may show divergent tissue combinations, i.e. they lack true osteodentin, never show 'hardened orthodentin', might have an outer collar of cellular (*Dasypus*) or acellular cementum (*Priodontes*, *Cabassous*, *Zaedyus*), or have an inner vasodentin core (*Dasypus*).

The combination of dentin varieties (and cementum) of differing biomechanical properties, mainly correlated with hardness, allows xenarthrans to develop a proper tooth relief depicting food choice and mastication movements (Fig. 12.1). Regarding function, xenarthrans with crushing-grinding dentitions show a forward directed jaw movement and gently sloped tooth relief (e.g., *Glyptodon*: Fig. 12.1A; *Lestodon*: Fig. 12.1B), contrasting strongly with xenarthrans with shear-cutting dentitions (e.g., *Euphractus*: Fig. 12.1D) showing a simpler vertical (open-close) jaw movement but pronounced tooth relief with cusps, valleys, and cutting edges. The latter occur as self-sharpening cutting blades, e.g., in the very large-bodied fossil ground sloths *Eremotherium* and *Megatherium* (Fig. 12.1C). The self-sharpening effect is achieved by considerable thinning of the orthodentin and orientation of the cutting blade perpendicular to the jaw movement. In addition, cheek teeth of *Megatherium* and *Eremotherium* show an especially dense meshwork of the odontoblastic process extensions.

Another peculiarity can be seen in species of the giant ground sloths *Scelidotherium*, *Lestodon*, *Glossotherium*, *Paramylodon*, and *Mylodon*. Microstructurally, the outer orthodentin portion shows fusion of five to fifteen individual dentinal tubules to cone-shaped bundles, each bundle raising slightly above the chewing surface. Raised parts are radially orientated and perpendicular to the outer margin of the tooth, thus having a washboard-like appearance. Although a functional interpretation does not suggest itself, the structure might have a positive effect on food processing. Morphologically similar structures are known from enamel in rhinoceros cheek teeth, here caused by a special microstructural arrangement of the enamel prisms (vertical Hunter-Schreger bands; Koenigswald 1997).

Dental microwear

Dental microwear depicts the relationship of the scaring of the chewing surface and the animal's last food items. Different techniques have been successfully employed to explore dietary adaptations in xenarthrans: scanning electron microscopy, stereomicroscopy, and confocal microscopy, each of them being different from the others in regard to magnification, area and parameters analyzed, and illumination (see references in Kalthoff & Green 2018), but all of them using orthodentin as target tissue. Green (2009a) used stereomicroscopy to categorize living armadillos and sloths in four dietary classes, namely folivore, folivore-frugivore, insectivore, and carnivore-omnivore, and evaluated in a follow-up study (Green 2009b) inter-tooth variations of microwear signals depending on tooth position and facet analyzed. Since then and with these prerequisites at hand, various fossil ground sloths have been analyzed in respect to their feeding ecology.

Two of the stratigraphically earliest definite sloths, *Octodontotherium grande* and *Orophodon hapaloides*, are known from the Late Oligocene of Patagonia, and

Fig. 12.2. Dentin microstructures in xenarthran cheek teeth. **A,** Glyptodontidae indet. (KOE 2879), longitudinal section, scanning electron micrograph. The subparallel oriented, calcified odontoblastic processes are densely packed and show short but strong side extensions. **B,** *Hapalops* sp. (KOE 3012), longitudinal section, scanning electron micrograph. In sloths, cheek teeth show an outer collar of tooth cementum (C), followed by a layer of orthodentin (Ord), and a layer of vasodentin (Vd) in the tooths' center. A crack in the vasodentin is filled by epoxy resin, appearing dark grey in the image. **C,** *Nothrotheriops texanus* (KOE 3053), transverse section, scanning electron micrograph. Detail of the orthodentin layer showing dentinal tubules with odontoblastic processes (OP); the orthodentin matrix consists of intertubular dentin (ITD), dentinal tubules are lined with the highly mineralized peritubular dentin (PTD). **D,** *Bradypus tridactylus* (KOE 3070), unprepared cheek tooth, three dimensional synchrotron radiation X-ray tomographic micrograph. Light grey color represent the densely spaced, peritubular dentin (PTD) filled dentinal tubules with the odontoblastic process (OP, black spot). Darker grey color surrounding the tubules represent intertubular dentin (ITD). **E,** Megatheriidae indet. (KOE 3003), longitudinal section, scanning electron micrograph. The calcified tubes of the odontoblastic processes show very long extensions, the latter forming a dense network. **F,** *Proeutatus* sp. (KOE 3425), transverse section, scanning electron micrograph. In a number of fossil cingulates, cheek teeth show a central, cloud-shaped core of osteodentin (Ostd), followed by a thick layer of orthodentin (Ord), and an outer rim of hardened orthodentin (HOrd). The orthodentin layer displays well preserved incremental lines. **G,** *Glyptodon clavipes* (KOE 3060), transverse section, µ-CT image. The tooth fragment shows the same built-up as described in (F), the hardened orthodentin (HOrd) is light-grey colored and thus optically more dense. KOE, Enamel collection, established by Wighart von Koenigswald, housed in the Institute of Geosciences, Section Paleontology, Rheinische Friedrich-Wilhelms-Universität Bonn.
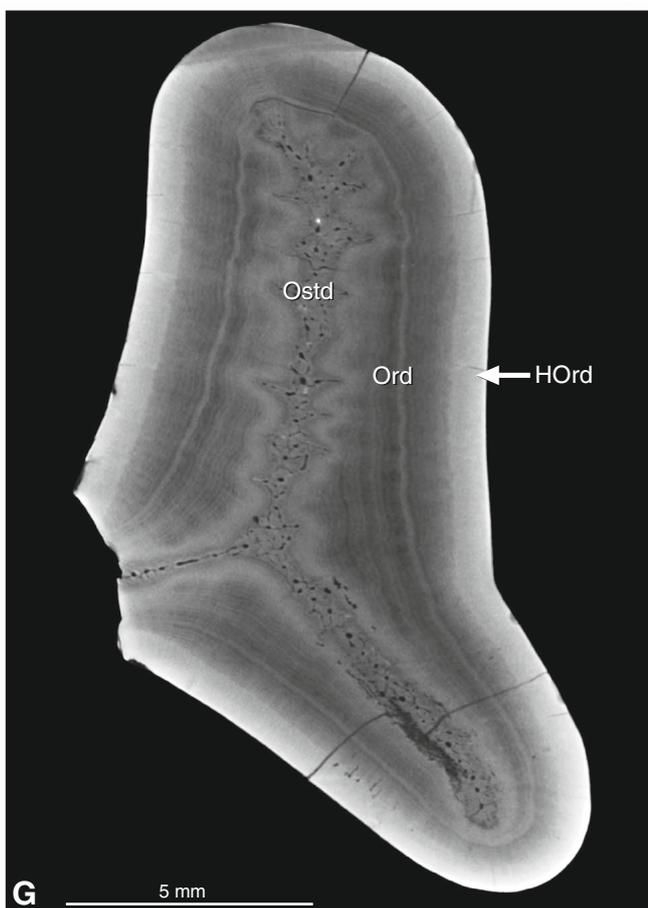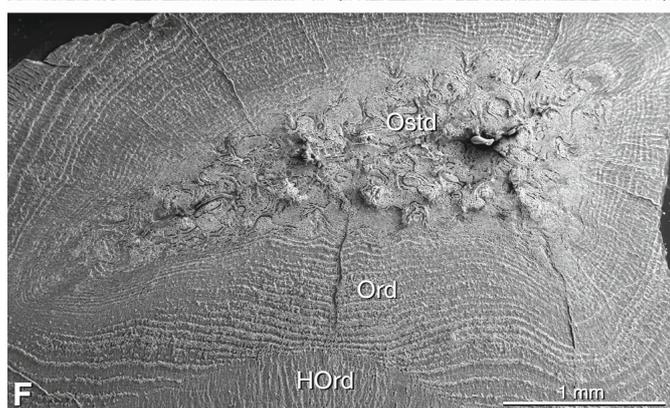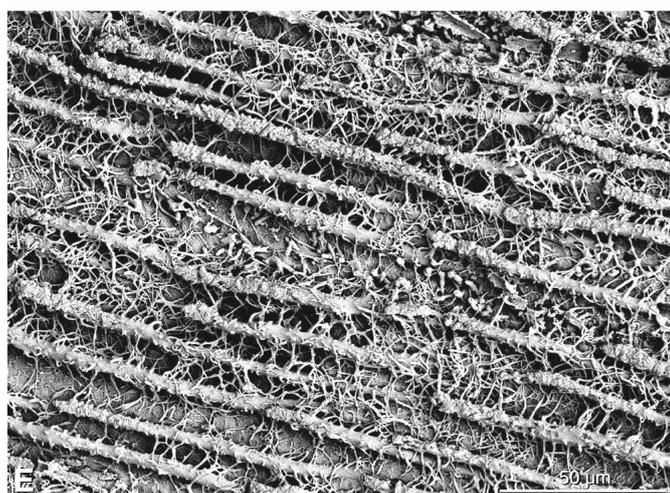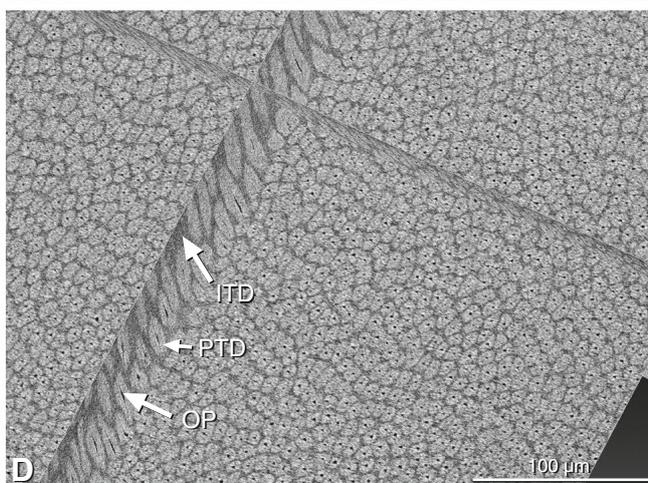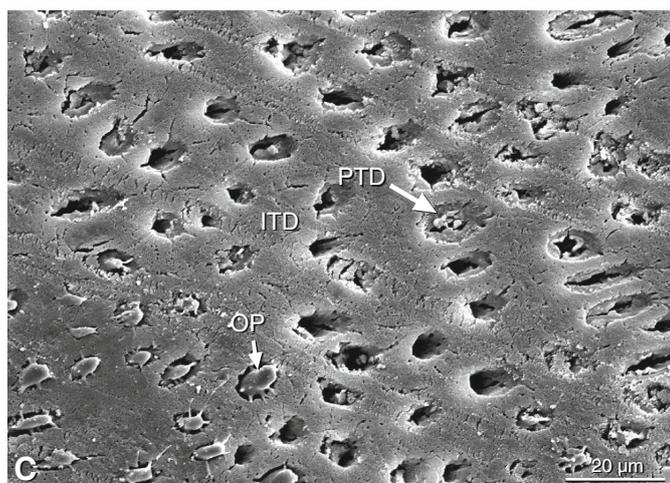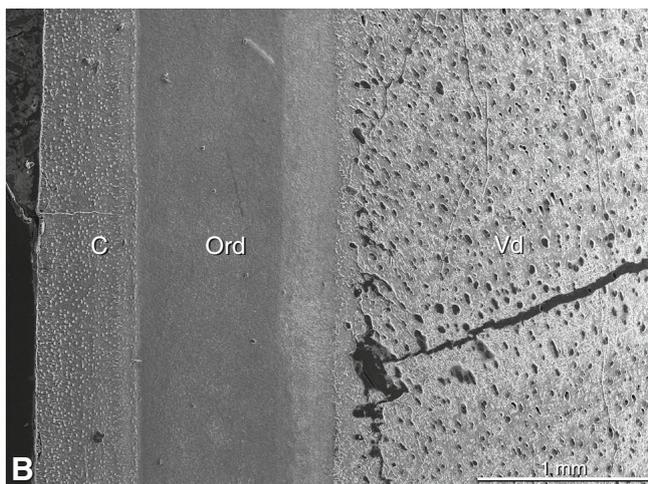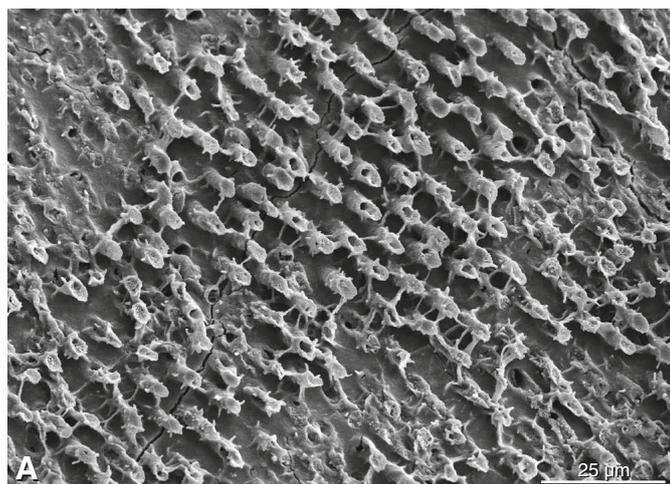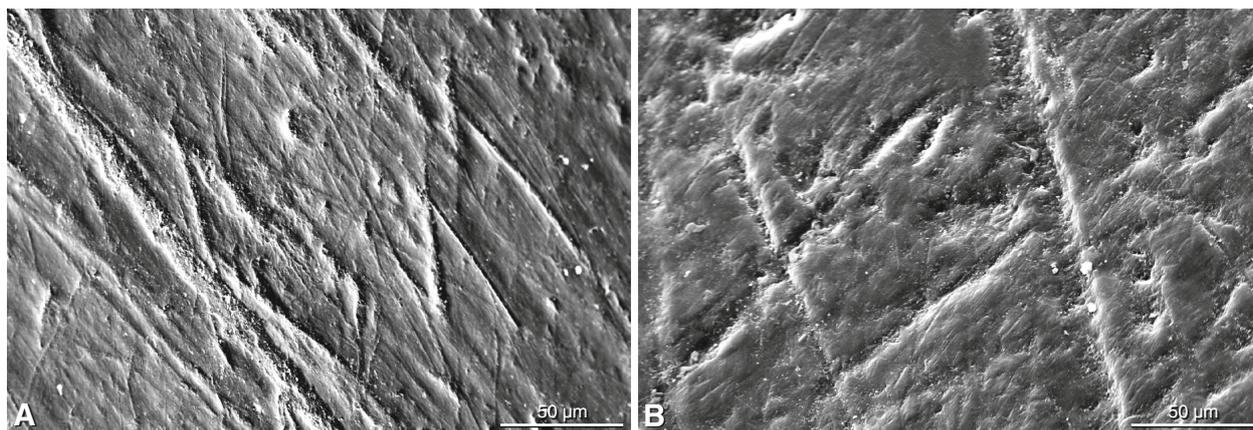
Fig. 12.3. Orthodentin surface of the stratigraphically earliest definite sloths showing representative microscopic scars. **A,** *Orophodon hapaloides* (MNHN.F.DES 267), right lower cheek tooth, scanning electron micrograph. **B,** *Octodontotherium grande* (MNHN.F.DES 238), right upper cheek tooth, scanning electron micrograph. Both wear surfaces display fine (i.e. narrow), coarse (i.e. wide), and hypercoarse (i.e. very wide scratches). Small (i.e. shallow) and large (i.e. deep) pits are scattered over the surfaces but not so easy to discern. MNHN: Muséum national d'Histoire naturelle, Paris.

systematically belong to the Mylodontoidea. Both species show microwear signals (Fig. 12.3), which are very different from all other analyzed sloths to date, both fossil and living. The results in Kalthoff & Green (2018) suggest a generalized herbivorous diet consisting of softer (foliage, fruit pulp) to harder (fruit, seeds, twigs) food items that were taken both from higher vegetation levels as well as from ground level. On the base of their wide muzzle, *Octodontotherium* and *Orophodon* are interpreted as so-called bulk feeders, meaning that the morphology and/or dimensions of their feeding apparatus prevents selective foraging; this is supported by their unspecialized, varied menu. In the early days of their evolution, sloths clearly were herbivorous but still unspecific in their food choice distinguishing them from both stratigraphically younger sloths and the living species, all of which are much more specialized in respect to their diet.

A number of Pleistocene ground sloths have been analyzed and compared to the living two- and three-toed sloths, i.e. the frugivore-folivore *Choloepus* and the folivore *Bradypus* (Green 2009a, Green & Resar 2012, Resar et al. 2013, Green & Kalthoff 2015). The Antillean sloth *Acratocnus odontrigonus* and the North American *Megalonyx wheatleyi* have pit-dominated microwear signals with *A. odontrigonus* falling in the dietary ecospace together with *Choloepus*, while *M. wheatleyi* falls between the latter and the all folivore *Bradypus*. A browsing behavior was also identified in the North American Shasta ground sloth *Nothrotheriops shastensis*, being in its food choice most similar to extant *Bradypus*. In contrast, the North American mylodontid *Thinobadistes segnis* and the giant ground sloth *Megatherium americanum* are characterized by scratch-dominated microwear signals, suggesting a more abrasive herbivorous diet comprising mature leafs, woody plants, and fruit. In both species, high scratching might be related to contamination of food items with grit, which is in accordance with habitat reconstructions suggesting a dryer, more open landscape, at least for *Megatherium* (Bargo 2001). These results fit well with the idea that large megatheriid sloths ecologically represented the "giraffe niche" (McDonald 2005) feeding in the higher levels of the canopy, in which dust particle accumulation might occur (Ungar et al. 2005).

The above results clearly show a dietary niche partitioning in Pleistocene ground sloths. However, only a fraction of their diversity has been analyzed to date, not to mention fossil cingulates, i.e. fossil Dasypodidae, Glyptodontidae, Pampatheriidae), for which microwear studies are currently unavailable. Much work remains to be done, and we have only opened a small window into the feeding ecology of fossil xenarthrans.

Summary

The monophyletic Xenarthra show a large number of unusual morphological synapomorphies distinguishing them from all other placental clades. Within toothed xenarthrans (sloths, armadillos, and their fossil relatives), their evergrowing, enamelless teeth with a layered composition of dentin varieties are unique. Each of these dentin varieties is identified by a specific microstructural make-up, representing different biomechanical properties from weaker (vasodentin) to strong (orthodentin) to very strong (hard orthodentin and osteodentin) capability of resistance against abrasion. These specific microstructural make-ups lead to diverse tooth reliefs, ranging from dentitions with lobed, rather shallow teeth having a predominant grinding function (e.g., Mylodontidae) to dentitions with bilophodont teeth having a predominant shear-cutting function (Megatheriidae). This result implies that the loss of the hard outer enamel layer has never been a drawback in the evolution and diversification of xenarthrans, probably due to hypselodonty and also relaxed selection on the dentition. Recent studies on the feeding ecology of extant and extinct

ground sloths revealed a variety of dietary adaptations along a line of specialized leaf browsing to more generalized browsing comprising also food items with a higher intrinsic toughness. They allow exciting insights into the biology of this clade and independent evidence for testing existing assumption on life history traits of fossil xenarthrans.

Acknowledgments

References

* indicates publications that originated from the DFG Research Unit 771.

Arsuffi, E. (1938): Beiträge zur Kenntnis des Vasodentins. Zeitschrift für Anatomie und Entwicklungsgeschichte 108: 749–760.

Bargo, M. S. (2001): The ground sloth *Megatherium americanum*: skull shape, bite forces and diet. Acta Palaeontologica Polonica 46: 173–192.

Bargo, M. S. & Nyakatura, J. A. (eds.) (2018): Special Issue: Morphology and Evolution of Xenarthra. Journal of Mammalian Evolution 25: 445–588.

Carlson, S. J. (1990): Vertebrate dental structures. In: Carter, J. G. (ed.). Skeletal Biomineralisation: Patterns, Processes and Evolutionary Trends. Vol. 1. Van Nostrand Reinhold, New York: 531–556.

Ciancio, M. R., Vieytes, E. C. & Carlini, A. A. (2014): When xenarthrans had enamel: insights on the evolution of their hypsodonty and paleontological support for independent evolution in armadillos. Naturwissenschaften 101: 715–725.

Fariña, R. A, Vizcaíno, S. F. & Iuliis, G. de (2013): Megafauna. Giant Beasts of Pleistocene South America. Indiana University Press, Bloomington.

Fariña, R. A, Vizcaíno, S. F. & Storch, G. (eds.) (2003): Morphological Studies in Fossil and Extant Xenarthra (Mammalia). Senckenbergiana Biologica 83: 1–101.

Ferigolo, J. (1985): Evolutionary trends in the histological pattern in the teeth of Edentata (Xenarthra). Archives of Oral Biology 30: 71–82.

Gotliv, B. A. & Veis, A. (2007): Peritubular dentin, a vertebrate apatitic mineralized tissue without collagen: Role of a phospholipid-proteolipid complex. Calcified Tissue International 81: 191–205.

Gotliv, B. A. & Veis, A. (2008): The composition of bovine peritubular dentin: Matching TOF-SIMS, scanning electron microscopy and biochemical component distributions. Cells Tissues and Organs 189: 12–19.

Green, J. L. (2009a): Dental microwear in the orthodentine of the Xenarthra (Mammalia) and its use in reconstructing the paleodiet of extinct taxa: the case study of *Nothrotheriops shastensis* (Xenarthra, Tardigrada, Nothrotheriidae). Zoological Journal of the Linnean Society 156: 201–222.

Green, J. L. (2009b): Intertooth variation of orthodentine microwear in armadillos (Cingulata) and tree sloths (Pilosa). Journal of Mammalogy 90: 768–778.

*Green, J. L. & Kalthoff, D. C. (2015): Xenarthran tooth architecture and dietary adaptations from analyses of dental microstructure and microwear, with new data for the giant sloth *Megatherium americanum* (Megatheriidae). Journal of Mammalogy 96: 645–657.

Green, J. L. & Resar, N. A. (2012): The link between dental microwear and feeding ecology in tree sloths and armadillos. Biological Journal of the Linnean Society 107: 277–294.

Habelitz, S., Rodriguez, B. J., Marshall, S. J., Marshall Jr, G. W., Kalinin, S. V. & Gruverman, A. (2007): Peritubular dentin lacks piezoelectricity. Journal of Dental Research 86: 908–911.

Haupt, R. J., DeSantis, L. R. G., Green, J. L. & Ungar, P. S. (2013): Dental microwear texture as a proxy for diet in xenarthrans. Journal of Mammalogy 94: 856–866.

Hoffman, J. M., Fraser, D. & Clementz, M. T. (2015): Controlled feeding trials with ungulates: a new application of in vivo dental molding to assess the abrasive factors of microwear. Journal of Experimental Biology 218: 1538–1547.

*Kalthoff, D. C. (2011): Microstructure of dental hard tissues in fossil and Recent xenarthrans (Mammalia: Folivora and Cingulata). Journal of Morphology 272: 641–661.

*Kalthoff, D. C. & Green, J. L. (2018): Feeding ecology in Oligocene mylodontoid sloths (Mammalia, Xenarthra) as revealed by orthodentine microwear analysis. Journal of Mammalian Evolution 25: 551–564.

*Kalthoff, D. C., Rose, K. D. & Koenigswald, W. v. (2011): Dental microstructure in *Palaeanodon* and *Tubulodon* (Palaeanodonta) and bioerosional tunneling as a widespread phenomenon in fossil mammal teeth. Journal of Vertebrate Paleontology 31: 1303–1313.

Kastelein, R. A. (2009): Walrus: *Odobenus rosmarus*. In: Perrin, W. F., Würsig, B. & Thewissen, J. G. M. (eds.). Encyclopedia of Marine Mammals (Second Edition). Academic Press in Elsevier, Burlington, San Diego, London: 1212–1217.

Keil, A. & Venema, B. (1963): Struktur und Mikrohärteuntersuchungen an Zähnen von Gürteltieren. Zoologische Beiträge 9: 173–195.

Koenigswald, W. v. (1997): Evolutionary trends in the differentiation of mammalian enamel ultrastructure. In: Koenigswald, W. v. & Sander, P. M. (eds.). Tooth Enamel Microstructure. Balkema, Rotterdam: 203–235.

Martin, B. E. (1916): Tooth replacement in *Dasypus novemcinctus*. Journal of Morphology 27: 647–682.

McDonald, H. G. (2005): Paleoecology of extinct xenarthrans and the Great American Biotic Interchange. Bulletin of the Florida Museum of Natural History 45: 313–333.

Meredith, R. W., Gatesy, J., Murphy, W. J., Ryder, O. A. & Springer, M. S. (2009): Molecular decay of the tooth gene enamelin (ENAM) mirrors the loss of enamel in the fossil record of placental mammals. PLoS Genetics 5: 1–12.

Mjör, I. A. & Nordahl, I. (1996): The density and branching of dentinal tubules in human teeth. Archive of Oral Biology 41: 401–412.

Murphy, W. J., Eizirik, E., Johnson, W. E., Zhang, Y. P., Ryder, O. A. & O'Brien, S. J. (2001): Molecular phylogenies and the origin of placental mammals. Nature 409: 614–618.

O'Leary, M. A., Bloch, J. I., Flynn, J. J., Gaudin, T. J., Giallombardo, A., Giannini, N. P., Goldberg, S. L., Kraatz, B. P., Luo, Z.-X., Meng, J., Ni, X., Novacek, M. J., Perini, F. A., Randall, Z. S., Rougier, G. W., Sargis, E. J., Silcox, M. T., Simmons, N. B., Spaulding, M., Velazco, P. M., Weksler, M., Wible, J. R. & Cirranello, A. L. (2013): The placental mammal ancestor and the post-K-Pg radiation of placentals. Science 339: 662–667.

Oliveira, E. V. (2001): Micro-desgaste dentario em alguns Dasypodidae (Mammalia, Xenarthra) [Dental microwear in some Dasypodidae]. Acta Biologica Leopoldensia 23: 83–91.

Owen, R. (1840–1845): Odontography; or, a Treatise on the Comparative Anatomy of the Teeth; their Physiological Relations, Mode of Development, and Microscopic Structure, in Vertebrate Animals. Hippolyte Bailliere, London.

Owen, R. (1842): Description of the Skeleton of an Extinct Gigantic Sloth, *Mylodon robustus*, Owen, with Observations on the Osteology, Natural Affinities, and Probable Habits of the Megatheroid Quadruped in General. Taylor, London.

Purnell, M., Seehausen, O. & Galis, F. (2012): Quantitative three-dimensional microtextural analyses of tooth wear as a tool for dietary discrimination in fishes. Journal of the Royal Society Interface 9: 2225–2233.

Rensberger, J. M. (1978): Scanning electron microscopy of wear and occlusal events in some small herbivores. In: Butler, P. M. & Joysey, K. A. (eds.). Development, Function, and Evolution of Teeth. Academic Press, New York: 415–438

Resar, N. A., Green, J. L. & McAfee, R. K. (2013): Reconstructing paleodiet in ground sloths (Mammalia, Xenarthra) using dental microwear analysis. Kirtlandia 58: 61–72.

Retzius, A. (1837): Bemerkungen über den inneren Bau der Zähne mit besonderer Rücksicht auf den in Zahnknochen vorkommenden Röhrenbau. Archiv für pathologische Anatomie und Physiologie und für klinische Medizin 1837: 486–566.

Schmidt, W. J. (1924): Über das Dentin von *Bradypus tridactylus*. Anatomischer Anzeiger 58: 97–107.

Schmidt, W. J. & Keil, A. (1958): Die gesunden und die erkrankten Zahngewebe des Menschen und der Wirbeltiere im Polarisationsmikroskop. Hanser, München.

Schöne, B. R., Dunca, E., Fiebig, J. & Pfeiffer, M. (2005): Mutvei's solution: An ideal agent for resolving microgrowth structures of biogenic carbonates. Palaeogeography, Palaeoclimatology, Palaeoecology 228: 149–166.

Semprebon, G. M., Godfrey, L. R., Solounias, N., Sutherland, M. R. & Jungers, W. L. (2004): Can low-magnification stereomicroscopy reveal diet? Journal of Human Evolution 47: 115–144.

Simpson, G. G. (1932): Enamel on the teeth of an Eocene edentate. American Museum Novitates 567: 1–4.

Teaford, M. F. (1991): Dental microwear: what can it tell us about diet and dental function. In: Kelley, M. A. & Larsen, C. S. (eds.). Advances in Dental Anthropology. Wiley-Liss, New York: 341–356.

Ten Cate, A. R. (1998): Oral Histology, 5th ed. Mosby, St. Louis.

Ungar, P. S., Teaford, M. F., Glander, K. E. & Pastor, R. F. (1995): Dust accumulation in the canopy: a potential cause of dental microwear in primates. American Journal of Physical Anthropology 97: 93–99.

Vizcaíno, S. F. & Loughry, W. L. (eds.) (2008): The Biology of the Xenarthra. University Press of Florida, Gainesville.

Walker, P. L. (1976): Wear striations on the incisors of cercopithecoid monkeys as an index of diet and habitat preference. American Journal of Physical Anthropology 45: 299–308.

Walker, A., Hoeck, H. N. & Perez, L. (1978): Microwear of mammalian teeth as an indicator of diet. Science 201: 908–910.

Winkler, D. E., Schulz-Kornas, E., Kaiser, T. M. & Tütken, T. (2019): Dental microwear texture reflects dietary tendencies in extant Lepidosauria despite their limited use of oral food processing. Proceedings of the Royal Society B 286. https://doi.10.1098/rspb.2019.0544

Appendix 1. Specimen details of the extinct and extant sloths mentioned in the text. Dietary adaptations follow Green (2009a), Resar et al. (2013), Green and Kalthoff (2015), and Kalthoff and Green (2018). Country codes refer to ISO 3166-1 alpha-2. Abbreviations: LMA, Land Mammal Age; m, lower molariform; M, upper molariform. For Acronyms of collections, see Appendix 2.

Taxon	Stratigraphical age/LMA
Mylodontidae	
Scelidotherium sp.	Pleistocene ("Pampeano")
Scelidotherium	Early Pleistocene (Ensenadense)
Mylodontidae indet.	No data
Mylodontidae indet.	Late Miocene-Pliocene (Mesopotamian)
Mylodon sp.	No data
Thinobadistes segnis	Miocene
Glossotherium robustus	Late Miocene/Early Pliocene ('Mesopotamiense')
Paramylodon harlani	Late Pleistocene (Rancholabrean)
Paramylodon harlani	Late Pleistocene (Rancholabrean)
Lestodon armatus	Early Pleistocene (Pampas inferior)
Octodontotherium sp.	?Late Oligocene (Deseadan)
Octodontotherium grande	Late Oligocene (Deseadan)
Orophodon hapaloides	Late Oligocene (Deseadan)
Megatheriidae	
Eremotherium eoimigrans	Early Pleistocene
Eremotherium laurillardi	Late Pleistocene
Megatheriidae indet., small (*Promegatherium* vel *Pliomegatherium* vel *Pyramiodontherium*)	Late Miocene-Pliocene
Megatheriidae indet.	Pleistocene
Megatheriidae indet.	No data
Megatherium americanum	Pleistocene
Nothrotheriidae	
Nothrotheriops shastensis	Late Pleistocene (Rancholabrean)
Nothrotheriops texanus	Early Pleistocene (Irvingtonian)
Megatheroidea indet.	
Hapalops sp.	Late Early Miocene (Santacrucian)
Megalonychidae	
Choloepus sp.	Recent
Acratocnus odontrigonus	Pleistocene
Megalonyx wheatleyi	Pleistocene
Bradypodidae	
Bradypus torquatus	Recent
Bradypus tridactylus	Recent

Sample provenance	Sample no.	Original coll. no.	Tooth position	Special dentin character	Diet based on dentin microwear
No data	KOE 3577	MLP 50-VIII-1-1	Probably M2	Cone-shaped bundles of dentinal tubules	
Entre Pto. de Olivos y Pta. Anchore, prov. Buenos Aires, AR	KOE 3433	MLP 54-VI-19-8	Molariform	Cone-shaped bundles of dentinal tubules	
No data	KOE 3004	AMNH 11282	Molariform	Cone-shaped bundles of dentinal tubules	
Paraná, prov. Entre Rios, AR	KOE 3432	MLP 41-XII-13-2080	Molariform	Cone-shaped bundles of dentinal tubules	
No data	KOE 3000	AMNH 132682	Molariform	Cone-shaped bundles of dentinal tubules	
Mixon's Bone Bed, Florida, US	–	AMNH FAM (2 teeth); FMNH (3 teeth)	molariforms (5) (2 MF, 3 mf)		Plants with low to moderate intrinsic toughness; possible influence of grit/dust
No data	KOE 3541	AMNH 11273	Molariform	Cone-shaped bundles of dentinal tubules	
Rancho La Brea, California, US	KOE 3569	LACMHC 130 757	Left M2	Cone-shaped bundles of dentinal tubules	
Rancho La Brea, California, US	KOE 3573	LACMHC 130 761	Right m2	Cone-shaped bundles of dentinal tubules	
Rio Arrecifes, AR	–	NHMD-ZMK 52/1888 (former ZMUC 154)	Right m1-3	Cone-shaped bundles of dentinal tubules	
Ez. Co. Alto. zona del Rio Deseado, Prov. Santa Cruz, AR	KOE 3434	MLP 52-XI-3-15, diverse numbers	Molariform	Small amount of central vasodentin	Generalized herbivorous diet; bulk feeding
La Flecha, Patagonia, AR	–	MNHN.F.DES	molariforms (9) (5 MF, 3 mf, 1 MF/mf)	Small amount of central vasodentin	Generalized herbivorous diet; bulk feeding
La Flecha, Patagonia, AR	–	MNHN.F.DES diverse numbers	molariforms (5) (2 MF, 3 mf)	Small amount of central vasodentin	Generalized herbivorous diet; bulk feeding
AL033: Haile 16A, Alachua Co., Florida, US	KOE 3044	UF 46361	Molariform	Strong thinning of orthodentin layer	
LV028: Waccassassa River, Levy Co., Florida, US	KOE 3045	UF 16416	Molariform	Strong thinning of orthodentin layer	
Paraná, Prov. Entre Rios, AR	KOE 3431	MLP 325	Molariform	Strong thinning of orthodentin layer	
Quebrada de Agua, ?AR	KOE 3003	AMNH 123683	Molariform	Strong thinning of orthodentin layer	
No data	KOE 3578	YPM 25011 PU	Molariform	Strong thinning of orthodentin layer	
"Plata-Landene" (territory of today's Argentina, Paraguay, Uruguay, and parts of Bolivia)	–	NHMD-ZMK 56/1885 (former ZMUC 19)	Molariform	Strong thinning of orthodentin layer	Plants with low to moderate intrinsic toughness; possible influence of grit/dust
Potter Creek Cave, California, US	–	UCMP 8141, 8336, 8704, 8715	molariforms (4) (all M2/M3)	Thinning of orthodentin layer	Herbivorous diet
HI007: Leisey Shell pit 1A, Hillsborough Co., Florida, US	KOE 3053	UF 87136	Molariform	Thinning of orthodentin layer	
Estancia La Costa, layer ?3, Prov. Santa Cruz, AR	KOE 3012	IGPB uncat.	Molariform		
No data	KOE 3590	SMF 35.784	Molariform		Frugivore – folivore
Puerto Rico, PR	–	AMNH	molariforms (3)		Frugivore – folivore
Smith Pit, Florida, US	–	AMNH	molariforms (6)		Folivore
No data	KOE 3018	ZSM 1903/9534	Molariform		Folivore
"Vivarium", supposedly from Ménagerie du Jardin des Plantes, Paris, FR	KOE 3070	MNHN CG 1954-268	Molariform		Folivore

Appendix 2. Specimen details of the extinct and extant cingulates mentioned in the text. Dietary categories follow Green (2009a). Country codes refer to ISO 3166-1 alpha-2.

Abbreviations: LMA, Land Mammal Age; M, upper molariform. Acronyms to museum collections: AMNH, American Museum of Natural History, New York, USA; FMNH, Field Museum of Natural History, Chicago, USA; IGPB, Institute of Geosciences, Section Paleontology, Rheinische Friedrich-Wilhelms-Universität Bonn, Bonn, Germany; KOE, Enamel collection, established by Wighart von Koenigswald, Institute of Geosciences, Section Paleontology, Rheinische Friedrich-Wilhelms-Universität Bonn, Germany; LACMHC, Los Angeles County Museum Hancock Collection (Page Museum), Los Angeles, USA; MACN, Museo Argentino de Ciencias Naturales "Bernardino Rivadavia", Buenos Aires, Argentina; MLP, Museo de La Plata, La Plata, Argentina; MNHN, Muséum national d'Histoire naturelle, Paris, France; NRM, Swedish Museum of Natural History, Stockholm, Sweden; NHMD, Natural History Museum of Denmark, Copenhagen, Denmark; NHMD-ZMK, Natural History Museum of Denmark: Quaternary Zoology collection, Copenhagen, Denmark; SMF, Senckenberg Forschungsinstitut und Naturmuseum Frankfurt, Germany; UCMP, University of California Museum of Paleontology, Berkeley, USA; UF, Florida Museum of Natural History, University of Florida, Gainesville, USA; YPM, Peabody Museum of Natural History, Yale University, New Haven, USA; ZMB, Museum für Naturkunde (Zoologisches Museum), Berlin, Germany; ZSM, Zoologische Staatssammlung München, Germany. Uncat.: uncataloged.

Taxon	Stratigraphical age/LMA	Sample provenance	Sample no.
Cingulata: Dasypodinae			
Dasypus hybridus	Recent	No data	KOE 3010
Dasypus novemcinctus	Recent	No data	KOE 3442
Dasypus novemcinctus	Recent	Golf Course near Friesenhahn Ranch, Texas, US	KOE 3534
Euphractinae			
Chaetophractus villosus	Recent	No data	KOE 3046
Chaetophractus villosus	Recent	No data	KOE 3441
Chlamyphorus truncatus	Recent	No data	KOE 3021
Euphractus sexcinctus	Recent	No data	KOE 3594
Euphractus sexcinctus	Recent	Lagoa Santa, Minas Gerais, BR	–
Eutatus seguini	Pleistocene ("Pampeano")	No data	KOE 3424
Macroeuphractus sp.	Pliocene	No data	KOE 3588
Proeutatus sp.	Late Early Miocene (Santacrucian)	Monte León, Santa Cruz, AR	KOE 3425
Zaedyus pichiy	Recent	Puerto Jenkins, Santa Cruz, AR	KOE 3022
Tolypeutinae			
Cabassous unicinctus	Recent	Ipitingua, Rio Acara, BR	KOE 3019
Priodontes maximus	Recent	El Cerro, Chiguitos, BO	KOE 3015
Tolypeutes matacus	Recent	La Urbana, Tapikiolé, lower Rio Pilcomayo, PY	KOE 3020
Peltephilidae			
Peltephilus ferox	Late Early Miocene (Santacrucian)	No data	KOE 3429
Pampatheriidae			
Pampatherium sp.	No data	No data	KOE 3002
Pampatherium sp.	Pleistocene ("Pampeano")	Algarrobo, Ptdo C. Casares, Buenos Aires province, AR	KOE 3426
Pampatherium (= *Holmesina*) *floridanus*	Early Pleistocene (Irvingtonian)	HI007: Leisey Shell pit 1A, Hillsborough County, Florida, US	KOE 3047
Vassallia minuta	Pliocene ("Araucanense")	Catamarca province, AR	KOE 3428
Glyptodontidae			
Propalaehoplophorinae indet.	No data	Santa Cruz province, AR	KOE 3436
Propalaehoplophorus australis	Late Early Miocene (Santacrucian)	Santa Cruz province, AR	KOE 3538
Glyptodontidae indet.	Early Pleistocene (Ensenadan)	Buenos Aires province, AR	KOE 2879
Glyptodontidae indet.	No data	No data	KOE 3430
Glyptodon sp.	No data	No data	KOE 3001
Glyptodon sp.	No data	South America	KOE 3535
Glyptodon reticulatus	Pleistocene	Tarija, BO	KOE 3026
Glyptodon clavipes	Pleistocene	Arroyo del medio, Pampa intermedio, AR	KOE 3060
Hoplophorus ornatus	Pleistocene	Pergamino, Province Buenos Aires, AR	KOE 3061

Original coll. no.	Tooth position	Special dentin character	Dietary catagory based on dentin microwear
MLP uncat.	Molariform	Milk tooth generaton with enamelled teeth; ?central vasodentin	
–	Molariform	Milk tooth generaton with enamelled teeth; central vasodentin	Insectivore
IGPB M-6357	Molariform	Milk tooth generaton with enamelled teeth; central vasodentin	Insectivore
MLP uncat.	Molariform	'Degenerated osteodentin'	
MLP uncat.	Molariform	'Degenerated osteodentin'	
ZSM AM/1125	Right M7 and M8		Insectivore
SMF 908	Molariform		Carnivore – omnivore
NHMD L62 (former ZMUC L62)	Skull and mandibles		Carnivore – omnivore
MLP 16-146	Molariform	Hard orthodentin; osteodentin	
FMNH P 14493	Molariform	'Degenerated osteodentin'	
MLP 67-X-31-1	Molariform	Hard orthodentin; osteodentin	
ZMB 48626	Molariform	'Degenerated osteodentin'	Carnivore – omnivore
ZSM 1910/252	Molariform		Insectivore
ZSM 1926/359	Right M3		
ZSM 1925/595	Molariform	'Degenerated osteodentin'	Insectivore
MLP 69-VIII-13-3	Molariform	'Degenerated osteodentin'	
–	Molariform	Hard orthodentin; osteodentin	
MLP 70-III-10-1	Molariform	Hard orthodentin; osteodentin	
UF 65890	Molariform	Hard orthodentin; osteodentin	
MLP 29-X-10-71	Molariform	Hard orthodentin; osteodentin	
MACN A-11229	Upper molariform	Hard orthodentin; osteodentin	
AMNH 132681	Molariform	Hard orthodentin; osteodentin	
–	Molariform	Hard orthodentin; osteodentin	
MLP s/n	Molariform	Hard orthodentin; osteodentin	
–	Molariform	Hard orthodentin; osteodentin	
AMNH 11301	Molariform	Hard orthodentin; osteodentin	
NRM-PZ M2519	Molariform	Hard orthodentin; osteodentin	
NHMD-ZMK 70/1885 (former ZMUC 109)	Molariform	Hard orthodentin; osteodentin	
NHMD-ZMK 77/1888 (former ZMUC 170)	Molariform	Hard orthodentin; osteodentin	